# Power Quality Enhancement in Standalone Microgrid Based On UPQC with coati optimized PR cascaded -PID controller

\*1Ratheesh, 2Jebavins

\*¹Chairman,
Maathangi Info Research Solutions Private Limited,
Marthandam, Tamil Nadu 629165, India.
\*Email: sratheeshtpm@gmail.com

<sup>2</sup>Senior Manager, Maathangi Info Research Solutions Private Limited, Marthandam, Tamil Nadu 629165, India. Email: jebavins.m1986@gmail.com

**Abstract:** The use of standalone microgrids (MG) has grown because to their greater flexibility in supplying energy based on customer needs and the growth in pollution. Integrating renewable energy sources (RES) with various loads will exacerbate the power quality challenges in MG. The primary goal of the proposed work is to reduce the power quality (PQ) issue in the MG by the unified PQ conditioner (UPQC) with the propotional resonant cascaded proportional integral derivative (PRc-PID) based on the coati optimization (COA). The fuel cell, solar cell, wind turbine and hydroelectric power are planned for the independent MG. To ensure optimal supply to the converter, UPQC shunt and series regulators employ a combination PRc-PID controller. PQ issues are overcome using UPQC in the system, and the efficiency of UPQC is increased by combining PRc-PID with a COA-based controller in series and a shunt active power filter to reduce current and voltage PQ issues. PQ concerns such as current and voltage are addressed utilizing a control mechanism to improve MG's stability and reliability. The Simulink platform will be used to implement the proposed work. The performance of the proposed work is confirmed by incorporating three cases into the system. The total harmonic distortion for the proposed model is 3.30%. Various PQ issues, like interruption, swell and sag, and harmonics, are examined.

Keywords: Power quality, microgrid, PI controller, UPQC, PID controller, coati optimized UPQC, active power filters.

#### 1. Introduction

Microgrid (MG) is the basic element that plays a significant role in the integration of RES [1, 2]. Due to its numerous benefits, the energy system is continuously evolving to bring benefits in multiple areas. Regardless of system variations, the MG components should be in the optimal range [3]. The MG can be controlled via three strategies: primary, secondary, and tertiary controls. Each controlling strategy is used for the source, modes of operation, and coordination. It should be noted that the operation of MG can be monitored by the primary and secondary control systems, while the tertiary control is on the utility grid [4].

The MG is connected to the utility grid under normal conditions and disconnected under faulty conditions. However, both modes of operation should be operated within a specific range. MGs are associated with the grid through power electronic converters, which are also important for RES integration. However, the higher switching frequency in these devices may destroy the PQ in the system [5]. The increasing demand for reliable operation of power grids has increased the demand for higher PQ [6]. PQ issues arise in a grid-connected PV system because to fluctuations in solar irradiation and the operation of power conditioning interface devices under light load conditions. Similarly, grid-connected wind energy systems suffer additional PQ issues, including as harmonics, inter-harmonics, voltage drops and swells, power outages, flickers, and phase imbalance. As a result, the issues have an impact on the overall efficiency of the energy system as well as the life of the electrical component. Advanced mitigation measures such as active power sorting, reactive power compensation, and adaptive control mechanisms are critical for enhancing power quality in microgrids powered by renewable energy [7].

Various filters and controllers have been used to improve system performance with different operations. On the other hand, the PQ problems are compensated by focusing on the inverter topology, the power conversion strategies and the inverter control mechanism. The optimization algorithm-based control solutions in [8] efficiently achieve PQ in MG. In [9], a symbiotic organism search method tunes the controller settings, which regulate voltage and frequency. Later, in [10], grasshopper optimization is applied to improve the dynamic response of grid-assisted power systems. In addition, voltage regulation [11] can be done through fuzzy-based

control by effectively controlling the battery. Furthermore, parallel active power filters (PAPF) and series APF (SAPF) are commonly utilized in systems to cancel current as well as voltage harmonics caused by irregular loads [12]. The combination of SAPF and PAPF is the best method for improving system operation, leading to UPQC [13]. At the same time, the compensation of UPQC is an important research topic in both PQ and energy management. More attention is paid to the unified PQ conditioners (UPQC) to alleviate the PQ problems in the distribution network [14, 15]. The UPQC has recently been upgraded with the inclusion of an additional controller to improve operation [16]. Furthermore, it has been applied in the medical field to address PQ deformation. To alleviate PQ difficulties in voltage and current waveforms, UPQC uses shunt and series compensators [17, 18]. According to these methods, the hybrid AC-DC MG implements a number of methods based on optimization algorithms to maximize the control gains. Biogeography-based optimization is used with the UPQC in a hybrid solar-wind-connected energy system to solve PQ problems [19]. Several methods for solving the problems of unbalanced voltage and frequency are presented in the literature. Satisfying the PQ requirements is quite difficult during load variation and fault conditions in multiple DG-connected systems [20]. However, local optimal trapping can occur with the above methods. This proposed method is used to overcome these PQ issues. The primary goals of the suggested designs are outlined below:

- To design the standalone MG PV, wind turbine (WT), hydro and fuel cells are used. According to the irradiance, wind speed and water flow, power is generated from PV, WT and hydro. Due to environmental factors, these sources will struggle to load conditions. In this case, it uses a fuel cell to deliver the power at the load requirement.
- PQ problems like swelling, sagging and harmonics in voltage as well as current signals occur due to the interrelated system. It will have an impact on the system's stability as well as reliability; however, it can be addressed by employing the UPQC device.
- A COA-based PRc-PID controller strategy has been developed on the UPQC device, which reduces PQ failures and load requirements. Harmonics in the system were analyzed for voltage and current connected to load under various cases.

The rest of this paper is prearranged as follows: section 2 clarifies related works for promoting the quality of this paper. Section 3 explains the detailed standalone MG with renewable energy method, UPQC device, controller and optimization method used in this method. The comparison of the various simulation results is explained in section 4. Section 5 concludes this method with future direction.

#### 2. Related works

This section offers a thorough overview of the literature on using different controllers and optimization techniques to address PQ disturbance in the power system.

Rajesh et al. [21] introduced a hybrid technique to increase PQ in a multi-source connected power system. This proposed model improves the PQ independent of the variation in reactive and active power flow. This controller, based on hybrid optimization, supplies the PI controller with the best active and reactive power for generating the standard d-q current signal. Here, the control parameters of the PI were chosen based on the error metrics. This suggested model was evaluated using different test cases that considered the response of solar PV. The proposed strategy was estimated using statistical parameter analysis.

Nafeh et al. [22] suggested the voltage stability improvement method using fuzzy-operated D-STATCOM to improve the PQ. This proposed method was studied on a renewable energy battery power system. The control loop provides a unity power factor, with DC voltage controlled by an external control loop and active current controlled by the internal control loop. In this Fuzzy PI, the error and the derivative of the d-q axis current values were given and then added together using the integrator to minimize the errors. The DSTATCOM was employed to keep the voltage within acceptable limits by measuring the difference between the reference and DSTATCOM voltages.

Hussien et al. [23] suggested an optimized PI-based autonomous MG to improve efficiency under a variety of operating circumstances. The RSM strategy used in this model brings the correlation in the response of the control parameters. Some of the key performance indicators have been assigned to the proposed RSM. The proposed model was tested in different scenarios, and the input weights for 6 PI controllers were studied for DGs. The results were determined with regard to the isolated operation and changing load conditions.

Sindi et al. [24] suggested an optimized PID to improve the performance of adaptive PQ compensators (APQC) in multiple MGs (MMG) connected power systems. This APQC consists of two compensators, TCSC in series and SPFC in shunt tuned by the dual controller. The multilevel errors were controlled by the PID controller tuned to receive the pulses for the voltage source inverter (VSI). The minimum performance error was considered an objective function. The proposed model was examined using different failure scenarios and multiple controllers.

Nima Khosravi et al. [25] suggested the modified UPQC (MUPQC) with multi-resonant PI (MR-PI) for the standalone AC-MG. In this proposed model, control parameters were selected using an optimization algorithm. A neural-clamped inverter module was installed to rectify the voltage and current harmonics. The MUPQC converter

was driven by the positive voltage sequence in the AC-MG using the algorithm used in this work. The control of voltage and current was based on the conversion of the reference frame.

Satapathy et al. [26] created a NARX-NN controller that effectively tackles the specific problem of power quality in the MG with classic PID and fuzzy-based PID controllers. They ensure stability under real-life conditions such as impedance and communication delay. This controller scalability is validated through a large-scale Simulink and the real-world processor in the loop (PIL) testing. Here, the complexity and the dependence on the extensive training data are notable changes.

Sanjenbam and Singh [27] improved the power quality of a three-phase system by incorporating a frequency-locked loop approach into the integrator-based observer. The hydro turbine-driven three-phase induction generator powered the standalone system, which supplied power to sensitive non-linear loads. In addition, a unified power quality converter was attached to increase power quality. To manage the load voltage, UPQC used a series voltage source converter.

Budiman et al. [28] introduced a suitable harmonic power flow approach that combines harmonic power flow with an optimization formulation for daily optimal planning of a grid-connected microgrid. The power quality was assessed using three indices: voltage imbalanced factor, voltage total harmonic distortion, as well as voltage magnitude. Based on the demand side management, a non-iterative mitigation scheme was proposed to avoid power quality indices violations.

Chankaya et al. [29] demonstrated power quality difficulties at the distribution system's end point using a grid-tied PV system. To maintain the stability of the DC bus, an equilibrium-optimized PI controller was used. As a result, the DC bus voltage fluctuation was decreased throughout the situation. The system control performs a variety of duties, including load balancing, active and reactive power regulation, harmonics reduction, as well as power factor correction.

Tiwari [30] presented an enhanced MPPT method for PV systems using various optimization techniques. Techniques like fuzzy logic controllers, modified GWO, and whale optimization algorithms were presented for the MPPT controller. Modified grey wolf optimization (GWO) is one of the greatest methods in the solar system due to its low fluctuation and quick response. Temperature and irradiance are taken into account as input variables, and the modified GWO algorithm is utilized to enhance the ideal voltages as output variables. Table 1 compares existing work based on renewable energy sources with their advantages and disadvantages.

Table 1: A literature survey

Reference	Method	Objectives	Tool	Advantage	Drawbacks
[21]	Hybrid bat search and moth flame optimization tuned PI	To improve PQ	Matlab	Improves the PQ in multiple DGs connected power system	Ignoring THD analysis
[22]	Fuzzy-tuned PI D for DSTATCOM	Energy management and to improve PQ	Matlab	Fluctuations in voltage get reduced under faulty conditions.	Performance gets affected under load variations.
[23]	Sunflower optimized PI	Autonomous operation of MG	Simulink	RSM strategy improves the correlation	Lower convergence
[24]	Puzzle optimized PID controlled APQC	Control of MMG	Simulink	Lower THD	Complex model
[25]	MUPQC with MR-PI	Reducing PQ issues in AC-MG	Simulink	MUPQC was reset based on grid power	Higher THD
[26]	NARX-NN; fuzzy-PID control; PID	Reduce the PQ issue	MATLAB/Simulink and TMS320	Power quality is enhanced effectively	The accuracy and effectiveness are heavily dependent on the training data.
[27]	Enhanced integrator-based	Improved power quality	Matlab/Simulink	Reactive power elimination,	High settling time

	observer using frequency-locked loop approach.	of the independent three-phase system.		current harmonics reduction and power factor	
[28]	Optimal harmonic power flow framework	Optimal scheduling of a grid-connected microgrid	Matlab	Lower total cost	Uncertainty and harmonics were very high
[29]	Equilibrium- optimized PI controller	Control power quality issues at the end of the distribution system	Matlab/Simulink	Balancing grid current, harmonics suppression and reactive power compensation	Not accurately tracking the maximum power
[30]	Modified grey wolf optimization algorithm	An enhanced MPPT method for PV systems using various optimization techniques	Matlab/Simulink	Reduced harmonics	High cost

Several approaches have been introduced in the literature to solve the above-mentioned issues. To address these problems, the flexible AC transmission system (FACTS) is typically employed. However, the working of FACTS devices such as UPQC may be affected by system harmonics due to load variations. As a result, an effective controller must be installed in the power system to maintain frequency as well as voltage deviation. Thus, the proposed work will focus on the optimum operation of UPQC using the optimized controller.

# 3. Proposed Methodology

The RESs and DG naturally lead to MG, which consists of generation, storage, and loads. The MG can offer many advantages to the system, such as energy efficiency, reliability, sustainability, and resilience. A standalone MG system has multiple power inputs, uncertain optimal scheduling, flexible system structure, and multiple power reliability requirements. The proposed block diagram for a standalone MG is shown in Figure 1.

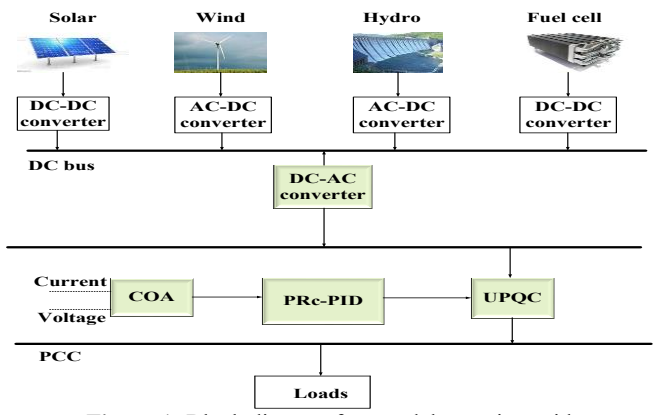


Figure 1: Block diagram for standalone microgrid

In this work, gird was divided into three parts: source, converter and PQ issues solver methods. Initially, RES like hydro, solar and wind are used as sources with a fuel cell. Voltages from these energy sources are converted to DC voltages using converters and related to the DC bus. The implementing method is kept between the alternate current bus and the point of common coupling. Between these, a UPQC is related to enhance the system's PQ. PRc-PID controller is connected instead of series and shunt active filters, respectively. The COA is utilized to tune the controlling parameter.

# 3.1 Solar PV modelling:

The solar PV is fundamentally a p-n junction fabricated on a thin semiconductor wafer. In solar energy, electromagnetic radiation can be converted directly into electricity via the photovoltaic effect [31]. The output power of PV is given below equation (1), (2) and (3):

$$A_{PV} = \eta_P A_{Pd} - \eta_P A_d \left[ \exp \left[ \frac{g \left( \frac{v_{PV}}{\eta_s} + L_s \frac{A_{PV}}{\eta_P} \right)}{ktC^N} \right] - 1 \right] - \frac{\left( \frac{\eta_s v_{PV}}{\eta_s} + AL_s \right)}{L_{sh}}$$

$$(1)$$

$$L_s(Total) = \frac{\eta_s L_s}{\eta_s} \tag{2}$$

$$L_{sh}(Total) = \frac{\eta_P L_s}{\eta_s} \tag{3}$$

Where  $\eta_s$  and  $\eta_P$  represent as similar cell and parallel cell.  $L_s$  and  $L_{sh}$  indicates the series and shunt resistance.  $v_{PV}$  and  $A_{PV}$  represent voltage as well as current of the photovoltaic cell as well as q represent charge produced in the system.

#### 3.2 Wind Turbine:

Wind turbine technology uses rotor blades to collect the kinetic energy of the wind as water flows. WT blades capture the wind's kinetic energy and transform it into mechanical energy [32]. The Mechanical power of this unit in equation (4):

$$P_{W} = \frac{1}{2} \rho \ C_{P} \pi R^{2} V_{W}^{3} \tag{4}$$

Where  $C_p$  represent the coefficient of performance,  $\rho$  specify air density,  $V_w$  indicates speed of wind and R is the blade length.

# 3.3 Fuel Cell:

A fuel cell is a device that converts chemical energy from fuel into electrical energy immediately [33]. This cell does not work like a battery because it does not store energy. Instead, it transforms energy from one state to another without consuming any materials in equation (5).

$$E_{\alpha} = N(E_n - in(I_0)) \tag{5}$$

Where,  $E_n$  signifies Nernst voltage and  $I_0$  represents the exchange current.  $E_\alpha$  represent the fuel cell and N represent the number of cells.

#### 3.4 Hydropower:

Hydro energy is obtained from flowing water by storing kinetic energy. Hydroelectricity is relatively cheap because it is an affordable and widely available resource. The energy that comes from moving water is called hydropower [34]. The size of the head and the water flow determine the amount of hydropower that can be produced from a hydro source. The hydro potential is expressed as equation (6):

$$P = \frac{1}{2} \rho A v^3 \tag{6}$$

Here, Area signifies the area of the hydropower, velocity is represented as V and density is denoted as  $\rho$ . These are the sources used to supply electric power to the standalone MG in this work.

# 3.5 Unified power quality conditioner:

A UPQC is a flexible tool that simultaneously reduces grid voltage disturbances as well as load current disturbances. The proposed MG system is built to operate loads using multiple feeders and linear loads. In UPQC, a custom power device connected between the feeders is used to mitigate the issues brought on by these various loads. Figure 2 depicts the design of the interline UPQC. This method combines a series and shunt APF connected together by a common DC link. Shunt active power filters are reconnected backwards, and the DC link is connected to a series of capacitors.

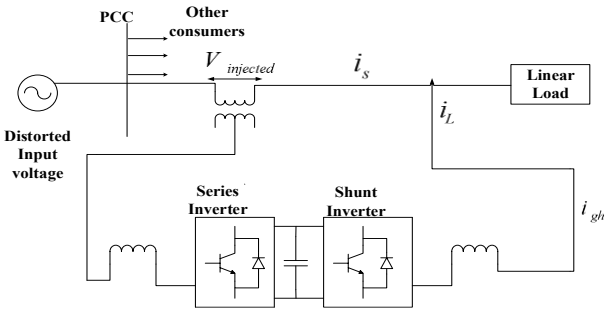


Figure 2: Line diagram of UPQC

Shunt converters are connected in parallel to series converters using point of common coupling (PCC). Series filters are used as voltage sources, while shunt filters are used as current sources in UPQC-arranged designs. UPQC can be used to overcome the PQ problems with current and voltage signals in standalone MG systems. There is no doubt that the shunt converters are employed on the supply side of the RES that mitigates the voltage spikes and the sag [26]. The series filter protects the system from voltage imbalances, flickering and other potential system threats while reducing harmonics at the transmission and distribution levels. In the case of a line fault caused by a high demand for reactive power or a voltage drop in the grid, the fixed-speed induction generator will fail and disconnect from the grid [35]. Implementing UPQC can be the greatest solution for integrating RES and grid while also protecting the system from voltage imbalances. This voltage drop leads to the turbine overspeeding; thus, the protection of the system becomes a major problem.

#### 3.5.1 Series Active Power Filter:

This type of active power filter is designed to rectify voltages. Input to the control block is intended to calculate instantaneous power PCC in phase voltage with line current compensation of non-linear loads. Three-phase voltage  $(V^{s(abc)})$  was altered before the d-q coordinates were created in the series active power filter controller given in equation (7).

$$\begin{pmatrix} V^{s0} \\ V^{sd} \\ V^{sq} \end{pmatrix} = \frac{2}{3} \begin{pmatrix} \frac{1}{2} & \frac{1}{2} & \frac{1}{2} \\ \sin(\omega t) & \sin(\omega t - \frac{2\pi}{3}) & \sin(\omega t + \frac{2\pi}{3}) \\ \cos(\omega t) & \cos(\omega t - \frac{2\pi}{3}) & \cos(\omega t + \frac{2\pi}{3}) \end{pmatrix} \times \begin{pmatrix} V^{sa} \\ V^{sb} \\ V^{sc} \end{pmatrix}$$

Three phase source voltage was described as  $V^{sa}$ ,  $V^{sb}$  and  $V^{sc}$ .  $V^{sq}$ ,  $V^{sd}$  is denoted for the quadrature axis and direct voltage. The equation (8) given below is used to find direct axis voltage.

$$V^{sd} = V^{sd} + \overline{V^{sd}}$$
 (8)

The below-mentioned equation (9) is used to compute the load voltage

$$\begin{pmatrix} VR^{1a} \\ VR^{1b} \\ VR^{1c} \end{pmatrix} = \frac{2}{3} \begin{pmatrix} \sin(\omega t) & \cos(\omega t) & 1 \\ \sin(\omega t - \frac{2\pi}{3}) & \cos(\omega t - \frac{2\pi}{3}) & 1 \\ \sin(\omega t + \frac{2\pi}{3}) & \cos(\omega t + \frac{2\pi}{3}) & 1 \end{pmatrix} \times \begin{pmatrix} \overline{V}^{sd} \\ 0 \\ 0 \end{pmatrix}$$
(9)

Voltage error is calculated by the equation (10);

$$E(V) = VR^{labc} - V^{sabc} \tag{10}$$

E(V) represent the voltage error,  $VR^{labc}$  represent the reference voltage and  $V^{sabc}$  represent the actual measured voltage.

### 3.5.2 Shunt Active Power Filter:

In a three-phase system without neutral, shunt power provides a portion of the oscillating active load current, resulting in a zero-powered zero-sequence component. The system's current harmonics are controlled using the instantaneous reactive power theory. The coefficients  $\alpha$  and  $\beta$  are used to translate three-phase voltage and current. Active and reactive power is designed using following equation (11);

$$\begin{pmatrix} P \\ Q \end{pmatrix} = \begin{pmatrix} V^{\alpha} & V^{\beta} \\ -V^{\beta} & V^{\alpha} \end{pmatrix} \begin{pmatrix} I^{\alpha} \\ I^{\beta} \end{pmatrix}$$
(11)

The reference current of shunt APF in  $\alpha$ - $\beta$  coordinates in equation (12) and (13),

$$\begin{pmatrix}
IR^{\alpha} \\
IR^{\beta}
\end{pmatrix} = \frac{1}{V_{\alpha}^{2} + V_{\beta}^{2}} \begin{pmatrix}
V_{\alpha} & V_{\beta} \\
-V_{\beta} & V_{\alpha}
\end{pmatrix} \begin{pmatrix}
\overline{p} - P_{0} + P_{loss} \\
0
\end{pmatrix}$$
(12)

$$E(I) = IR^{sabc} - I^{labc} \tag{13}$$

E(I) used to compute the error current in the method. After comparing these reference source current signals, three-phase source currents are detected. The hysteresis band PWM controller processes the errors to produce necessary switching signals for shunt APF switches. Here,  $V^{\alpha}$ ,  $V^{\beta}$ :  $\alpha$ ,  $\beta$  are the components of source voltage,  $I^{\alpha}$ ,  $I^{\beta}$ :  $\alpha$ ,  $\beta$  are the components of source current, P represent instantaneous active current and Q represent the reactive power. Where E(I) represent the error current,  $IR^{sabc}$  represent the reference current and  $I^{labc}$  illustrates the load current.

#### 3.6 PRc-PID controller:

Ideal PR controller performs with an infinite quality factor in a network, but it is a challenge to implement. Initially, neither an analogue nor a digital system can achieve the immeasurable quality factor produced by the PR controller's infinite gain [37]. Finally, the gain of the PR controller decreases significantly at other frequencies.

$$G_{PR}(s) = K_{p1} + K_{I1} \frac{2\omega_c s}{s^2 + 2\omega_c s + \omega_0^2}$$
 (14)

Where,  $G_{PR}(s)$  is the PR current controller,  $K_{II}$  represent integral gain term,  $K_{pl}$  indicates proportional gain term,  $\omega_c$  signifies bandwidth around the frequency of  $\omega_0$  and  $\omega_0$  is the resonant frequency. PR controller can be rendered less than the best value in order to avoid these issues by introducing damping, as shown in equation (14). The ac frequency  $\omega_0$  is finite with the gain of the PR controller in equation (14). When designing cascade controllers, the dynamics of the inner and outer loops must be separated. It is common for the inner loop to be faster than the outer. However, it is insufficient to eliminate harmonic effects caused by grid voltages; therefore, PID is integrated with this controller. It determines an error value as a variation from the measured process. The control inputs are adjusted to reduce the error for maintaining a variable and desired set point [36]. In terms of a control signal, error signal, the input-output relationship of a conventional continuous time linear PID controller in equation (15),

$$G_{PID}(t) = K_{p2}^{ct} e(t) + K_{I2}^{ct} \int_{0}^{t} e(\tau) d\tau + K_{D}^{ct} \frac{de(t)}{dt}$$
 (15)

Where,  $K_{p2}^{ct}$ ,  $K_{I2}^{ct}$  and  $K_{D}^{ct}$  represent gains of the CTLPID controller in terms of proportional, integral as well as derivative gain. Based on a mathematical model, PID is a linear controller with little flexibility. Using this controller makes it difficult to implement an effective non-linear power system. A cascaded PR and PID controller will resolve these difficulties in the MG.

PRc PID controllers diminish voltage and current in series and shunt active power filters in this work. PRc PID controllers are usually considered general versions of traditional PID controllers. The PID method takes advantage of high steady-state accuracy. This solves the problem of finding minor steady-state errors in the PR. The independent MG oscillations were reduced to a minimum by the PRc PID controller.

$$G_{PR_cPID}(s) = K_{p1} + K_{I1} \frac{2\omega_c s}{s^2 + 2\omega_c s + \omega_0^2} + K_{p2}^{cl} e(t) + K_{I2}^{cl} \int_0^t e(\tau) d\tau] + K_D^{cl} \frac{de(t)}{dt}$$
 (16)

Equation (16) represent the PR cascaded PID controller where it is given by  $G_{PR_cPID}(s)$ . The parameters  $K_{p1}$ 

,  $K_{I1}$ ,  $K_{p2}^{ct}$ ,  $K_{I2}^{ct}$  and  $K_{D}^{ct}$  of the controller are adjusted with the help of the coati optimization. The COA is one of the high-end optimization tools that is used for controlling purposes.

#### 3.7 Coati Optimization Algorithm (COA):

The proposed method uses the COA to reduce the current and voltage deviation in a standalone MG system with series and shunt controllers. Disruption, harmonics, sag interruption and swell, are the PQ issues in the entire MG. PQ issues are harmful to system performance, including dependability and stability. Shunt and series regulators detect variations in current and voltage in loads. DC-link capacitor can adjust for these variations when a UPQC device is connected. The UPQC device's dc-link voltage control responsibility is critical to the MG's reliable operation. The PRC-PID controller receives various voltages and currents. COA is an optimization approach that

achieves the optimum outcome while minimizing errors. General protocol, as well as recommended procedures, are covered in this section.

# 3.7.1 COA background information:

The coatis engage in intelligent behaviour when pursuing and evading predators and attacking and killing iguanas. The primary source of design inspiration for the suggested COA approach was the simulation of these coati's natural behaviour. The value of the function serves as the benchmark for candidate solution quality in metaheuristic algorithms like the proposed COA. The population member (gain parameter) is referred to as the best population. Randomly initialize the position of coati's in search space by the below equation (17):

$$X_{i}: X_{ij} = lb_{j} + r.(ub_{j} - lb_{j})$$

$$i = 1, 2, ...., N$$

$$j = 1, 2, ...., m$$
(17)

Here, N represent amount of coati's, m indicates the decision variable, r signifies random real number,  $X_i$ 

is  $i^{th}$  position of coati in search space and  $X_{ii}$  represent the value of  $j^{th}$  decision variable. In COA, the coati population is a mathematically represented population matrix. The below matrix shows the population matrix in equation (18) and (19):

$$X = \begin{bmatrix} X_{1} \\ \vdots \\ X_{i} \\ \vdots \\ X_{N} \end{bmatrix}_{N \times m} = \begin{bmatrix} X_{1,1} & \cdots & X_{1,j} & \cdots & X_{1,m} \\ \vdots & \ddots & \vdots & \ddots & \vdots \\ X_{i,1} & \cdots & X_{i,j} & \cdots & X_{i,m} \\ \vdots & \ddots & \vdots & \ddots & \vdots \\ X_{N,j} & \cdots & X_{N,j} & \cdots & X_{N,m} \end{bmatrix}_{N \times m}$$

$$F = \begin{bmatrix} F_{1} \\ \vdots \\ F_{i} \\ \vdots \\ F_{N} \end{bmatrix}_{N \times 1} = \begin{bmatrix} F(X_{1}) \\ \vdots \\ F(X_{N}) \end{bmatrix}_{N \times 1}$$

$$(18)$$

$$F = \begin{bmatrix} F_1 \\ \vdots \\ F_i \\ \vdots \\ F_N \end{bmatrix} = \begin{bmatrix} F(X_1) \\ \vdots \\ F(X_i) \\ \vdots \\ F(X_N) \end{bmatrix}$$
(19)

Where,  $F_i$  specifies value of the obtained objective function is based on  $i^{th}$  coati as well as F represent vector of objective function. The position of possible solutions in decision variables results in the estimation of various parameters for problems [38]. The fitness function for designing the controllers with different parameters is calculated to produce a less objective function. Multiple functional objective types exist because of the error in time dependence. The different types of fitness functions are represented in the equation (20) and (21).

$$IAE = \int_0^\infty |e(t)| dt \tag{20}$$

The integral of time multiplied absolute error (ITAE):

$$ITAE = \int_0^\infty t |e(t)| dt \tag{21}$$

Mathematical modelling of COA is classified into 2 methods based on coati's behaviour. (i) Strategy when attacking iguanas and (ii) escape plan from predators. In this strategy, when attacking iguanas, some coatis will climb the tree to reach an iguana. This method moves coatis to various locations within the search region, exhibiting the COA's ability to conduct global searches inside the problem-solving domain. As a result, the coati's location is initialized using the following equation (22).

$$X_i^{p1}: X_{i,j}^{p1} = X_{ij} + r.(Iguana_j - I.)X_{ij}$$
 (22)

 $X_i^{p1}$  updated location of the current solution in the dimension j for the individual i.  $X_{ii}$  represent the solution often for the best solution in the leader position. r represent the random number (0 to 1) for the introduction of the stochastic behaviour. Iguana, represent the fitness value. I. inertia factor possibility for the representation of the previous influence. Coatis on the ground move in the search space as an erratic location is simulated utilizing the following equation (23):

$$X_{i}^{p1}: X_{i,j}^{p1} = \begin{cases} X_{i,j} + r.(Iguana_{j}^{G} - 1.X_{i,j}), F_{iguana_{j}^{G}} < F_{i} \\ X_{i,j} + r.(X_{i,j} - Iguana_{j}^{G}), else \end{cases},$$
(23)

$$fori = \left\lfloor \frac{N}{2} \right\rfloor + 1, \left\lfloor \frac{N}{2} \right\rfloor + 2, \dots, N$$
 (24)

$$X_{i} = \begin{cases} X_{i}^{P1}, & F_{i}^{P1} \\ X_{i} & else. \end{cases}$$
 (25)

Iguana  $_{j}^{G}$  represent the position of an elite agent in the dimension j,  $F_{iguana}^{G} < F$  represent fitness value of

the elite agent than the current coati guided by the update and  $F_i$  represent the fitness of the current coati i. N

represent the total number of agents and  $\left\lfloor \frac{N}{2} \right\rfloor$  represent the ceiling function that rounds up to the integer. When

the updated process results in the different positions being considered for each coati, the value of the objective function in equation (24) increases and is updated in equation (25). In escaping predators' steps, coatis' positions get updated in terms of escaping from the hunters. The random position is generated near each coati location to imitate the behaviour based on equations (24) and (25).

$$lb_{j}^{bcal} = \frac{lbj}{t}, ub_{j}^{bcal} = \frac{ub_{j}}{t}$$

$$(26)$$

$$X_{i}^{p2}: X_{i,j}^{p2} = X_{i,j} + (1-2r)(lb_{j}^{bcal}) + r.(ub_{j}^{bcal} - lb_{j}^{bcal})$$
(27)

lbj and  $ub_j$  represent original lower as well as upper bound for the j dimension.  $lb_j^{bcal}$  and  $ub_j^{bcal}$  scaled bound at time t. A COA iteration is complete once the position in the search space is updated based on two phases. The population update involves equations (26) and (27). When a COA execution concludes, the best resolution for the algorithm is obtained as an output. Different steps involved in COA implementation are shown in Figure 3.

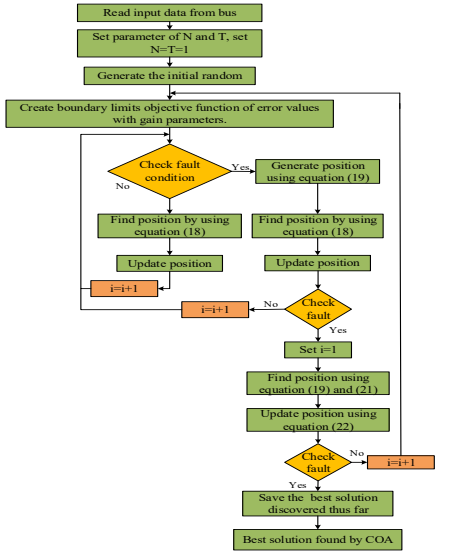


Figure 3: Flowchart of COA

Initially, a random placement of coati's is generated by using error values based on voltage and current. The position of each coati determines the current and voltage error minimization. This COA approach to global optimization problems offers a number of advantages. The design of this algorithm does not involve a control parameter; therefore, control parameters are not necessary. It is highly effective in solving complex, high-dimensional problems and a number of optimization problems in different fields. This proposed approach demonstrates excellent research and search process balancing capabilities. COA has strong performance in dealing with real-life situations.

# 4. Simulation Results:

In this section, several cases with outcomes are discussed. To evaluate the suggested approach's performance, simulation is carried out using the Simulink environment. Figure 4 demonstrations Simulink projection for implemented work with controller and optimization. In this work, PQ problems are reduced by using controller and optimization methods. This work shows a PQ improvement by reducing the THD when applying the fault.

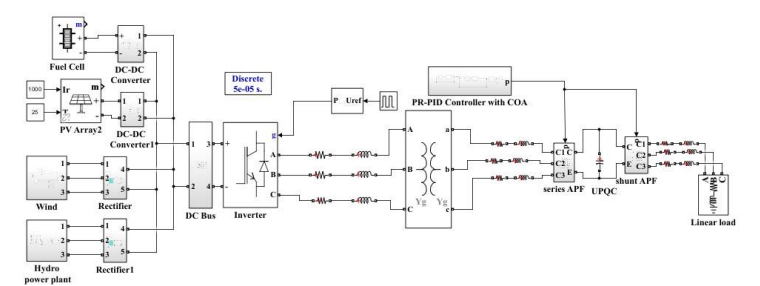


Figure 4: Simulink model for the proposed work

Table 2: Implementation Parameters

S. No	Description	Parameters	Values
1		Irradiance	1000
2	PV	Temperature	25 C
3		Generated power	1000W
4		Base Torque	200/0.9 N/m
5		Base rotational speed	1.2 m/s
6	WT	Nominal mechanical output power	750W
7		Armature inductance	0.000835
8		Base wind speed	12 m/s
9		Stator resistance	2.85 p. u.
10	Hydro	Nominal power	750W
11		Line-line voltage	13800
12		Number of cell	65
13	Fuel cell	Nominal stock effect	55%
14		Operating temperature	65 C
15		Number of iteration	100
16		Upper bond	100
17	COA	Lower bond	-100
18		Number of Population	30
19		Dimension	30

The performance is assessed by measuring the current and voltage with waveforms that are injected, compensating and creating problems. Comparing the proposed controller with other controllers will show better performance. Different PQ issues like harmonics, sag, and swell are used to validate the proposed controller with optimization. In this work, PQ is measured by comparing the THD under different cases, as well as by occurring sag and swell while applying fault in the inputs. For high PQ, the voltage ranges between two accurate voltmeters are also compared, measuring similar system voltage under different cases. Four instances are assessed to show the stability and reliability of the controller, which are tuned with optimization. Four cases are listed below:

Case 1: Source constant with Sag condition

Case 2: Source constant with Swell condition

Case 3: Disturbance and Interruption condition

Three separate scenarios are used to assess the effectiveness of the suggested approach. In the first scenario, the source remains constant in the Sag state. In the second situation, the Source is held constant by the Swell condition, whereas in the third case, the disturbance and interruption are considered. The electricity required to meet demand is provided by the hydro, PV and WT systems. These scenarios are detailed below, along with a design presentation. Table 2 demonstrations the parameters utilized for standalone MG and COA implementation.

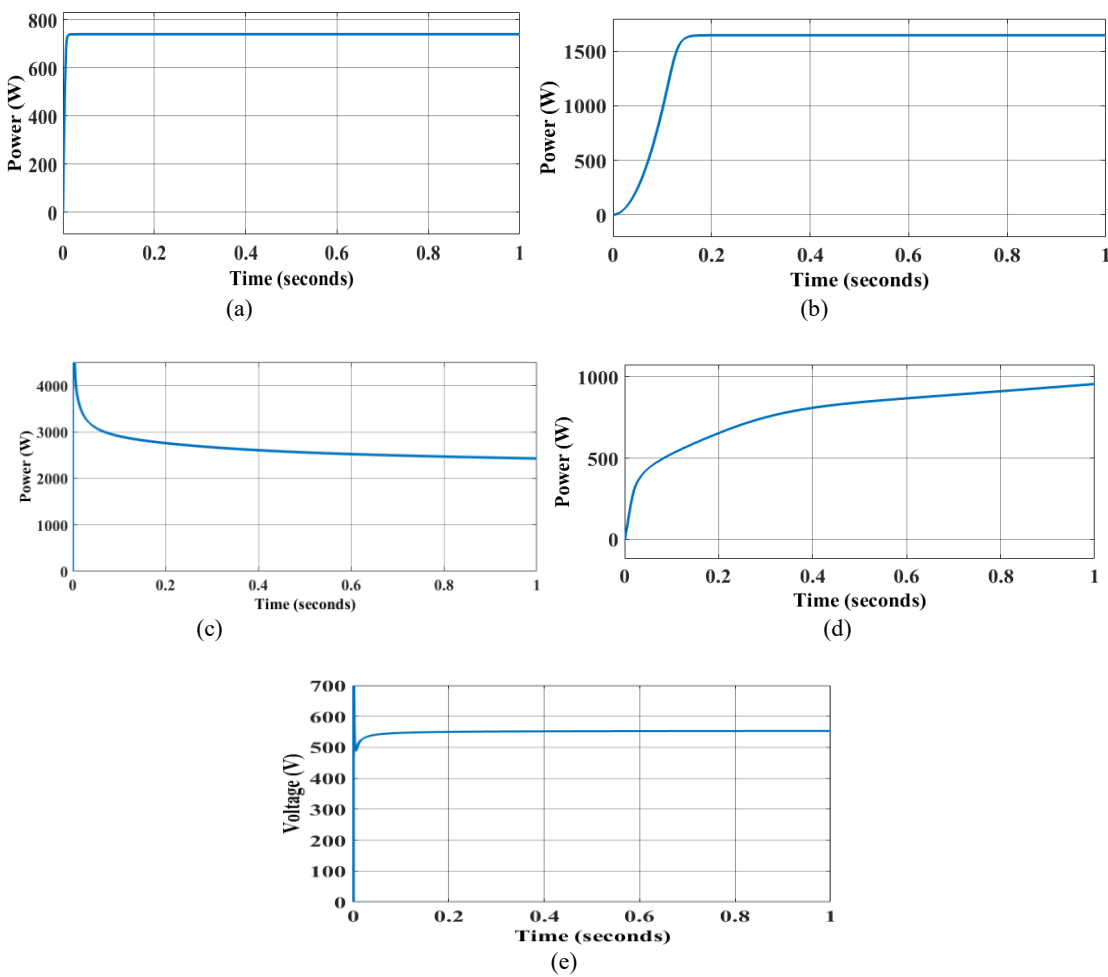


Figure 5: Power waveform for (a) fuel cell (b) PV (c) wind (d) hydro (e) DC link voltage

Figure 5 represents the output waveform for the fuel cell, PV, wind, hydro and DC link voltage for the suggested method. The proposed system adopts the combination of hybrid renewable energy resources (HRES) and the DC link voltage sources. Due to the environmental conditions, these sources are affected because they depend on natural resources to provide power. Irradiance, wind speed, and water flow conditions are set as constant. If Hydro, WT and PV fail to meet demand, fuel cells will offer the important power to the load. When wind turbines and PV supply excess energy, the fuel cell stores this energy for future use. To decrease the PQ problems, the UPQC controller is employed with the source as the input, and the result with different conditions is obtained in the proposed system.

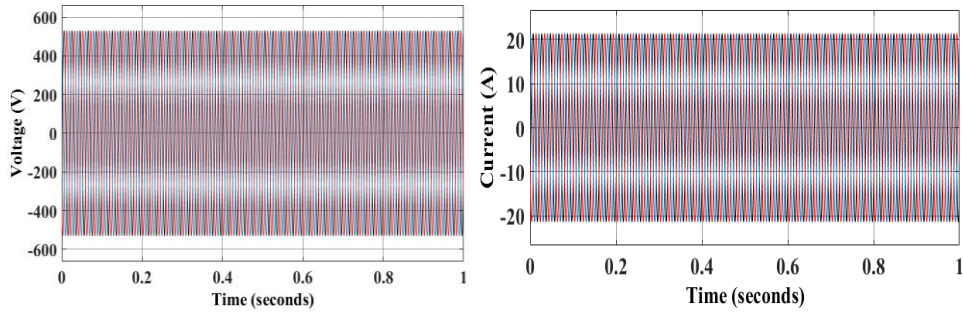


Figure 6: Inverter voltage and current

Figure 6 represents the output waveform for the voltage and current in the inverter. The inverter is also known as the converter, which is used to convert the DC source to an AC source. The grid-connected inverter is used to reduce power loss and increase the system's performance. The conversion efficiency is high, and the THD obtained is also low.

Case 1: Source constant with Sag condition

The verification of the predicted controller in the independent microgrid system is investigated using the sag situation. The most common causes of power quality issues include linked nonlinear, unbalanced, as well as critical loads. These load systems cause source side sag, which is handled in order to increase the stability and dependability of a standalone motor generator. In this condition, the source side fault causes the Sag, which is the suggested controller of the UPQC.

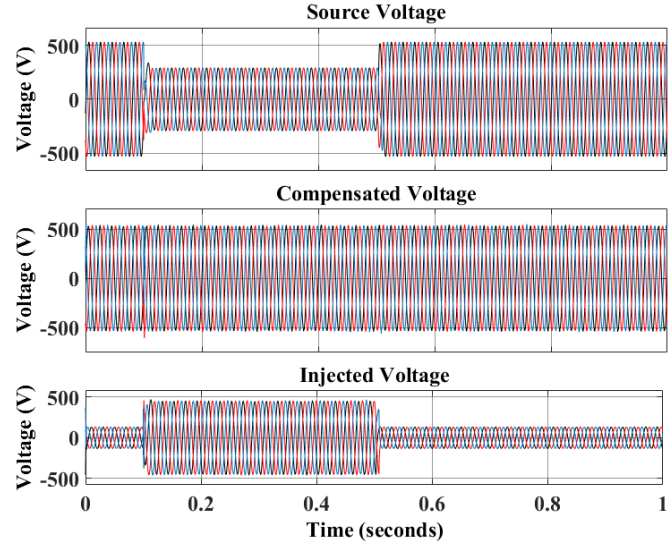


Figure 7: waveform of voltage Sag

Figure 7 represents output waveform for the voltage sag for the constant source for the system performance. Where the RES are considered as the source, they may be affected by the environmental condition due to the dependency on the natural resources to demonstrate the amount of power to the load. In this system, the irradiance and the wind speed are kept at  $1000 \text{W/m}^2$  and 12 m/s. The voltage sag developed in the standalone microgrid in the linear load. Figure 7 represents the voltage sag for the source, compensated and injected.

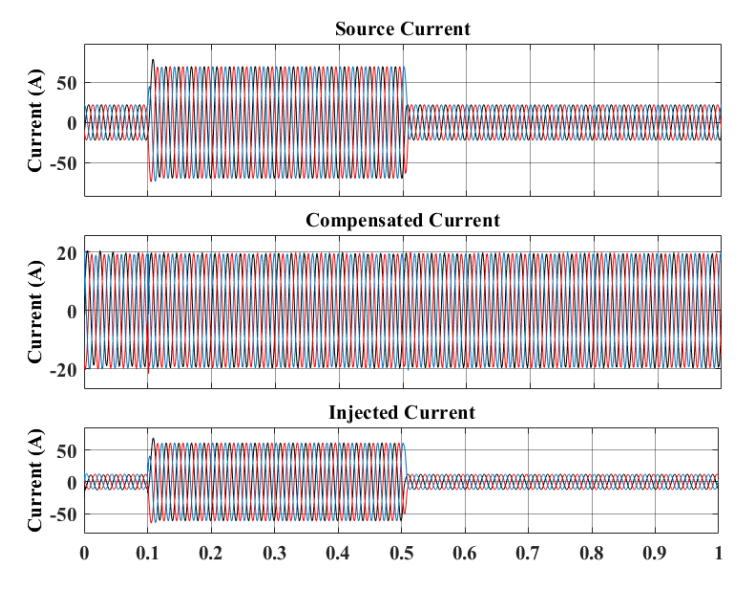


Figure 8: waveform of current Sag

Figure 8 represents output waveform for the Sag current in the constant source of the proposed system. The constant, compensated and injected current with respect to time is implemented in the proposed system. The compensated region shows a steady output form.

Case 2: Source constant with Swell condition

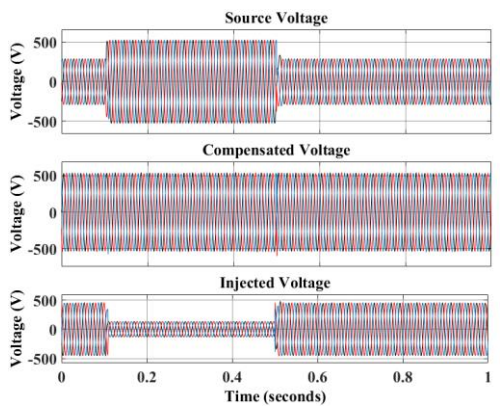


Figure 9: waveform of voltage Swell

Figure 9 represents the output waveform for voltage swell conditions used in the performance of the suggested controller. The RES demonstrate a stable condition, which is used to take the result in the standalone condition. The PQ issues in the Swell are adopted by applying a constant source condition; they are evaluated by the UPQC and the proposed PQ theory. The variation in the voltage system is taken from the source, compensated, and injected voltage. The compensated voltage is able to provide the system with its full potential.

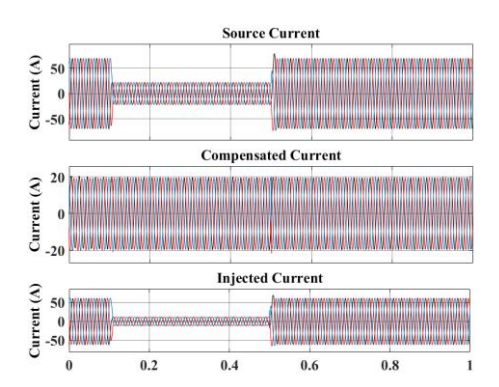


Figure 10: waveform of current swell

Figure 10 represents the output waveform for the current swell for the constant source system. The linear load conditions are introduced in the standalone microgrid system. The current swell waves with the introduction of the MG system in a linear load are supplied in the topology. To run the linearity and stability, the current swell needs to be evaluated in the system. Figures 8 and 9 show the decreases in the voltage and current swell condition with the help of the PQ theory and the UPQC.

Case 3: Disturbance and Interruption Condition

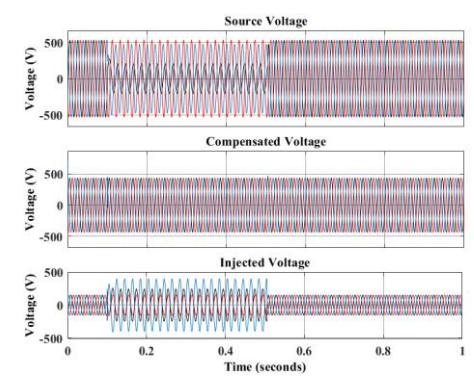


Figure 11: Analysis of disturbance and interuption for voltage condition in standalone microgrid

The third case brings the analysis of disturbance and Interruption for the voltage condition in the standalone MG. The analysis of the suggested method is done with the help of the controller. The disturbance and the interruption are obtained in the input region with the RES source. In order to counter this, novel converters are used in the system to reduce the disadvantages. Figure 11 represents the voltage stability in the disturbance and the interruption topology.

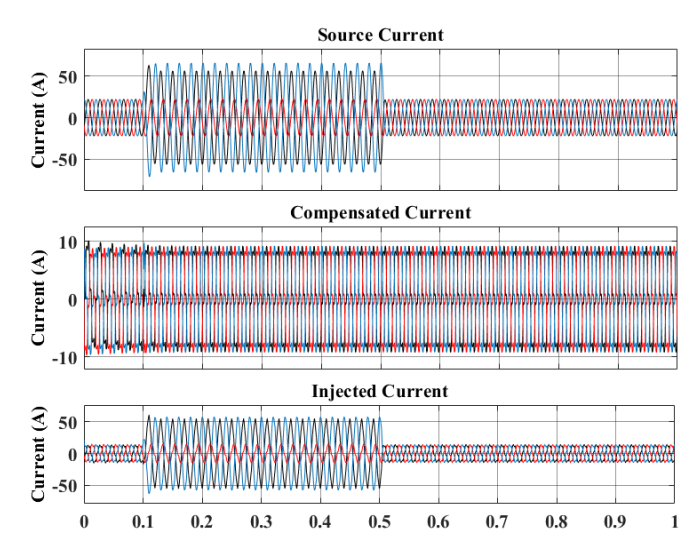


Figure 12: Analysis of disturbance and interruption for current condition in standalone microgrid

Figure 12 represents the analysis of the disturbance and interruption in the current condition in the standalone MG. In order to maintain stability, series and active power factors are employed in the system to reduce the PQ. The controllers play a major role in controlling the PQ. The injected system controls the disturbance and the interruption to resolve the power quality issues.

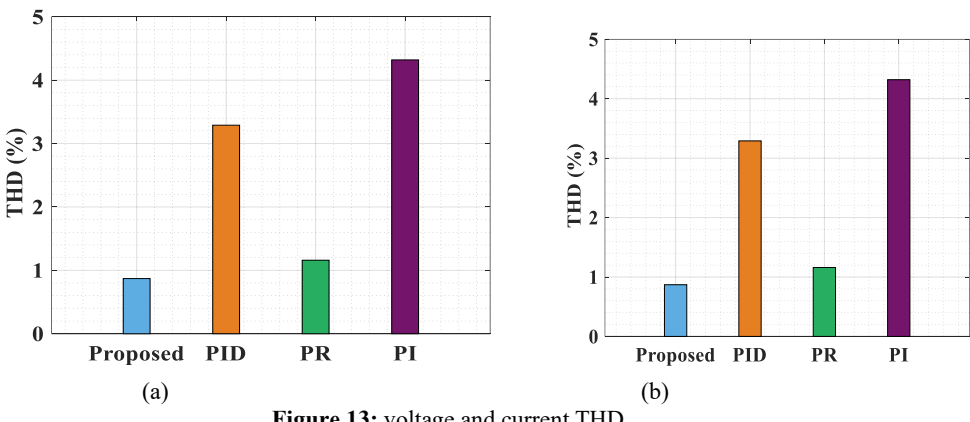


Figure 13: voltage and current THD

The THD comparison for the different controllers is introduced in the system. Figure 13 gives the voltage and current THD. The existing method was used to evaluate the THD and compare it with the predicted method. The suggested method is related with the PID, PR, and PI controllers, and it was found that the proposed system gives less THD. The values for different methods of optimization with respect to different parameters are depicted in Table 3.

Table 3: Comparison of different algorithm with different parameter

abic 5. Con	iparison of an	ilerent algorit	iiiii witti tiiit	Tent paramete
	Parameters			
Methods	kp	Kr	ki	kd
proposed	0.021794	0.284094	0.006606	0.169053
OOA	13.31099	8.146795	12.29033	7.669441
PSO	4.332115	6.552126	4.614348	1.98914
GWO	0.011089	0.008208	0.011402	0.008414

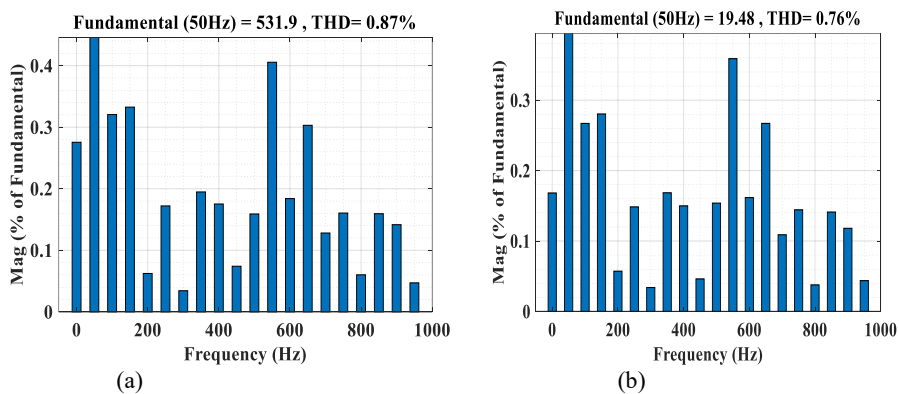


Figure 14: waveform of voltage and current THD

Figure 14 depicts the output waveform for the voltage and current THD. The harmonic distortion for the voltage is obtained to be 0.87% and the current to be 0.76%. The THD obtained is less when compared with the other topology. This brings the full performance of the proposed topology.

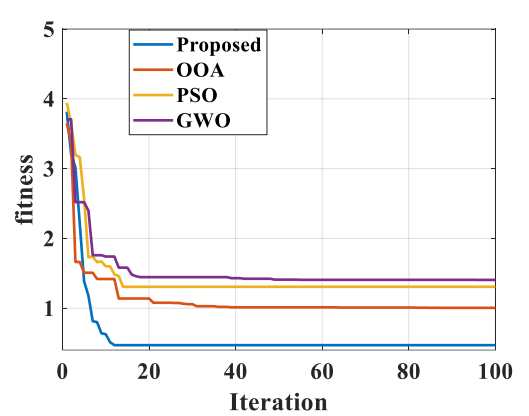


Figure 15: Comparison of convergence

Figure 15 compares the convergence curve for the optimization by demonstrating the proposed approach in resolving the 500 iterations with less fitness function. However, the optimal solution cannot be entirely resolved with the current approaches. With respect to other optimizations such as the proposed method, PSO, GWO and OOA, the proposed method achieves less iteration of the 14<sup>th</sup> iteration value of 0.4699 compared to other optimizations.

#### 5. Conclusion:

This paper proposes COA-based UPQC for a standalone MG system to reduce PQ issues. PV, WT, hydro and fuel cells are involved in the standalone MG design. On the load side, renewable energy systems are used to make up for necessary demand. PQ issues may impact how RES are linked to connected load systems. The UPQC with COA method was used to solve PQ problems in MG. This proposed method can improve the PQ issue in the standalone MG. An algorithm based on COA improves the performance of the PRc-PID controller by choosing the best pulses. The proposed controller evaluates several PQ issues like interruption, sag, swell and disturbance. The THD analysis was carried out for PI-PID and PRc-PID controllers, as well as for PRc-PID with COA. Compared with the two controllers, the THD value of the proposed method was 3.30%, and the PQ was improved by this method. According to the findings, the proposed UPQC with COA and PRc-PID controller achieves the greatest results for PQ mitigation. In the future, intelligent control algorithms can be applied to enhance the efficiency of three-phase UPQCs.

#### References

- [1]. Khosravi N, Echalih S, Baghbanzadeh R, Hekss Z, Hassani R, Messaoudi M (2022) Enhancement of power quality issues for a hybrid AC/DC microgrid based on optimization methods. IET renewable power generation vol. 16, no. 8, pp. 1773-91.
- [2]. Hirsch A, Parag Y, Guerrero J (2018) Microgrids: A review of technologies, key drivers, and outstanding issues. Renewable and sustainable Energy reviews vol. 90, pp. 402-11.
- [3]. Elmetwaly AH, ElDesouky AA, Omar AI, Saad MA (2022) Operation control, energy management, and power quality enhancement for a cluster of isolated microgrids. Ain Shams Engineering Journal vol. 13, no. 5, pp. 101737.

- [4]. Elmetwaly AH, Eldesouky AA, Sallam AA (2020) An adaptive D-FACTS for power quality enhancement in an isolated microgrid. IEEE Access vol. 8, pp. 57923-42.
- [5]. Thomas D, D'Hoop G, Deblecker O, Genikomsakis KN, Ioakimidis CS (2020) An integrated tool for optimal energy scheduling and power quality improvement of a microgrid under multiple demand response schemes. Applied energy vol. 260, pp. 114314.
- [6]. Hannan MA, Tan SY, Al-Shetwi AQ, Jern KP, Begum RA (2020) Optimized controller for renewable energy sources integration into microgrid: Functions, constraints and suggestions. Journal of Cleaner Production vol. 256, pp. 120419.
- [7]. Lavanya V, Kumar NS (2018) A review: Control strategies for power quality improvement in microgrid. International Journal of Renewable Energy Research vol. 8, no. 1, pp. 1-6.
- [8]. Rao SN, Kumar YV, Pradeep DJ, Reddy CP, Flah A, Kraiem H, Al-Asad JF (2022) Power quality improvement in renewable-energy-based microgrid clusters using fuzzy space vector PWM controlled inverter. Sustainability vol. 14, no. 8, pp. 4663.
- [9]. Teekaraman Y, Kuppusamy R, Nikolovski S (2019) Solution for voltage and frequency regulation in standalone microgrid using hybrid multiobjective symbiotic organism search algorithm. Energies vol. 12, no. 14, pp. 2812.
- [10]. Jumani TA, Mustafa MW, Md Rasid M, Hussain Mirjat N, Hussain Baloch M, Salisu S (2019) Optimal power flow controller for grid-connected microgrids using grasshopper optimization algorithm. Electronics vol. 8, no. 1, pp. 111.
- [11]. Behera S, Choudhury NB (2022) Modelling and simulations of modified slime mould algorithm based on fuzzy PID to design an optimal battery management system in microgrid. Cleaner Energy Systems vol. 3, pp. 100029.
- [12]. Mahdi DI, Gorel G (2022) Design and control of three-phase power system with wind power using unified power quality conditioner. Energies vol. 15, no. 19, pp. 7074.
- [13]. Rao RR, Pragaspathy S (2022) Enhancement of electric power quality using UPQC with adaptive neural network model predictive control. In2022 international conference on electronics and renewable systems (ICEARS) pp. 233-238. IEEE.
- [14]. Kumar CP, Pragaspathy S, Karthikeyan V, Prakash KD (2021) Power quality improvement for a hybrid renewable farm using UPQC. In2021 International Conference on Artificial Intelligence and Smart Systems (ICAIS) pp. 1483-1488. IEEE.
- [15]. Iqbal A, Waqar A, Madurai Elavarasan R, Premkumar M, Ahmed T, Subramaniam U, Mekhilef S (2021) Stability assessment and performance analysis of new controller for power quality conditioning in microgrids. International Transactions on Electrical Energy Systems vol. 31, no. 6, pp. e12891.
- [16]. Bakir H, Kulaksiz AA (2020) Modelling and voltage control of the solar-wind hybrid micro-grid with optimized STATCOM using GA and BFA. Engineering Science and Technology, an International Journal vol. 23, no. 3, pp. 576-84.
- [17]. Arulkumar T, Chandrasekaran N (2022) Development of improved sparrow search-based PI controller for power quality enhancement using UPQC integrated with medical devices. Engineering Applications of Artificial Intelligence vol. 116, pp. 105444.
- [18]. Samal S, Hota PK, Barik PK (2020) Performance improvement of a distributed generation system using unified power quality conditioner. Technology and Economics of Smart Grids and Sustainable Energy vol. 5, pp. 1-6.
- [19]. Goud BS, Rao BL, Flah A, Bajaj M, Sharma NK, Reddy CR (2022) Biogeography-based optimization for power quality improvement in HRES system. InPower Electronics and High Voltage in Smart Grid: Select Proceedings of SGESC 2021 pp. 309-316. Singapore: Springer Nature Singapore.
- [20]. Jumani TA, Mustafa MW, Alghamdi AS, Rasid MM, Alamgir A, Awan AB (2020) Swarm intelligence-based optimization techniques for dynamic response and power quality enhancement of AC microgrids: A comprehensive review. IEEE Access vol. 8, pp. 75986-6001.
- [21]. Rajesh P, Shajin FH, Umasankar L (2021) A novel control scheme for PV/WT/FC/battery to power quality enhancement in micro grid system: a hybrid technique. Energy Sources, Part A: Recovery, Utilization, and Environmental Effects pp. 1-7
- [22]. Nafeh AA, Heikal A, El-Sehiemy RA, Salem WA (2022) Intelligent fuzzy-based controllers for voltage stability enhancement of AC-DC micro-grid with D-STATCOM. Alexandria Engineering Journal vol. 61, no. 3, pp. 2260-93.
- [23]. Hussien AM, Hasanien HM, Mekhamer SF (2021) Sunflower optimization algorithm-based optimal PI control for enhancing the performance of an autonomous operation of a microgrid. Ain Shams Engineering Journal vol. 12, no. 2, pp. 1883-93.
- [24]. Sindi HF, Alghamdi S, Rawa M, Omar AI, Elmetwaly AH (2023) Robust control of adaptive power quality compensator in Multi-Microgrids for power quality enhancement using puzzle optimization algorithm. Ain Shams Engineering Journal vol. 14, no. 8, pp. 102047.
- [25]. Khosravi N, Echalih S, Hekss Z, Baghbanzadeh R, Messaoudi M, Shahideipour M (2022) A new approach to enhance the operation of M-UPQC proportional-integral multiresonant controller based on the optimization methods for a standalone AC microgrid. IEEE transactions on power electronics vol. 38, no. 3, pp. 3765-74.
- [26]. Satapathy A, Nayak N, Parida T (2022) Real-time power quality enhancement in a hybrid micro-grid using nonlinear autoregressive neural network. Energies vol. 15, no. 23, pp. 9081.
- [27]. Sanjenbam CD, Singh B (2024) Power quality enhancement of standalone hydropower generation system through modified integrator based observer controlled UPQC. Electric Power Systems Research vol. 226, pp. 109941.
- [28]. Budiman FN, Ramli MA, Bouchekara HR, Milyani AH (2024) Optimal scheduling of a microgrid with power quality constraints based on demand side management under grid-connected and islanding operations. International Journal of Electrical Power & Energy Systems vol. 155, pp. 109650.
- [29]. Chankaya M, Naqvi SB, Hussain I, Singh B, Ahmad A (2024) Power quality enhancement and improved dynamics of a grid tied PV system using equilibrium optimization control based regulation of DC bus voltage. Electric Power Systems Research vol. 226, pp. 109911.
- [30]. Tiwari A (2024) Improved power quality based PVDG system using different optimised MPPT controllers. Physica Scripta vol. 99, no. 2, pp. 025250.

- [31]. Gutiérrez-Martín F, Díaz-López JA, Caravaca A, Dos Santos-García AJ (2024) Modeling and simulation of integrated solar PV-hydrogen systems. International Journal of Hydrogen Energy vol. 52, pp. 995-1006.
- [32]. Yessef M, Bossoufi B, Taoussi M, Lagrioui A, Chojaa H (2022) Overview of control strategies for wind turbines: ANNC, FLC, SMC, BSC, and PI controllers. Wind Engineering vol. 46, no. 6, pp. 1820-37.
- [33]. Amatoul FZ, Er-raki M (2023) Modeling and simulation of electrical generation systems based on pem fuel cell-boost converter using a closed loop PI controller. Energy Reports vol. 9, pp. 296-308.
- [34]. Lescano JC, Junior LG, Souza HC, Estrabis T, Gentil G, Cordero R (2022) Modeling and Simulation of a Hydrokinetic Generation Connected to the Electricity Grid. InCongresso Brasileiro de Automática-CBA vol. 3, no. 1.
- [35]. Ravi T, Kumar KS, Dhanamjayulu C, Khan B, Rajalakshmi K (2023) Analysis and mitigation of PQ disturbances in grid connected system using fuzzy logic based IUPQC. Scientific Reports vol. 13, no. 1, pp. 22425.
- [36]. Joseph SB, Dada EG, Abidemi A, Oyewola DO, Khammas BM (2022) Metaheuristic algorithms for PID controller parameters tuning: Review, approaches and open problems. Heliyon vol. 8, no. 5.
- [37]. Priyadarshini S, Alam A, Shekhar S (2024) Design Of PI and PR controller in Various Reference Frames for Inverter Control. In2024 1st International Conference on Innovative Sustainable Technologies for Energy, Mechatronics, and Smart Systems (ISTEMS) pp. 1-6. IEEE.
- [38]. Kusuma PD, Dinimaharawati A (2023) Extended stochastic coati optimizer. International Journal of Intelligent Engineering and Systems vol. 16, no. 3, pp. 482-94.